

constant, i.e.,

$$k \approx k_- \ll k_+ \quad \text{or} \quad k \approx S_0 \ll k_+,$$

and k is small, $\sim 10^4$ dyn/cm.

In conclusion, the optical force constants of dielec-

tric solids depend strongly on the amount of covalent bonding between neighboring atoms. This covalent dependence may be described in terms of Pauling's theory of the chemical bond or parameters in the shell model of lattice vibration.

Direct Measurement of the Oxygen Vacancies Produced in Calcium Tungstate by Fast Reactor Neutrons*

K. C. CHU† AND C. KIKUCHI

Department of Nuclear Engineering, University of Michigan, Ann Arbor, Michigan 48105

(Received 13 December 1967)

The present paper is intended to point out the usefulness of electron spin resonance for the direct measurement of defect concentration. Fast-neutron irradiation results in a variety of paramagnetic centers in calcium-tungstate single crystals. From the g tensors, the hyperfine interaction, and the result of a uniaxial-stress experiment, one of the centers has been identified as due to paramagnetic tungsten associated with a displaced nearest-neighbor oxygen. The concentration of oxygen displacements is measured by comparison with a copper-sulfate standard and is calculated using the Kinchin-Pease theory. The measured and calculated values are in good agreement.

I. INTRODUCTION

ONE of the fundamental problems in the study of radiation effects is the determination of the concentration of the defects. Even though many physical properties are changed by radiation, very few techniques provide an opportunity for direct measurement of the defect concentration. Besides the problem of identification of defects, the basic difficulty is that the dependence of changes in various properties due to the introduction of defects is not understood well enough theoretically to provide reliable methods for an absolute determination of defect concentrations.

One method, used successfully by Antal, Weiss, and Dienes,¹ employs the transmission of long-wavelength neutrons (beyond the Bragg cutoff of the crystal) through irradiated solids. This technique, however, is limited to materials of low neutron-capture cross section. The minimum detectable concentration of defects is governed by the available neutron intensity, the capture cross section, and the bound-atom coherent scattering cross section of the atoms of the solid. To date, only concentrations of the order of 0.1% or greater have been detected. This requires a very high integrated fast-neutron flux, of the order of 10^{19} to 10^{20} nV.

The second method of direct measurement of defect concentration was introduced by Levy.² Using un-

strained single crystals of sodium chloride, Levy observed that all the negative-ion vacancies were converted to stable F centers following a γ -ray dose of about 10^7 R. If crystals were subsequently exposed for a time to reactor irradiation, he found that upon resumption of the γ irradiation, the F -center concentration increased in proportion to the integrated fast-neutron flux. The measured defect concentration due to fast neutrons was in agreement with radiation-damage theory. The determination of defect concentration requires additional information about the oscillator strength of the F centers.

When paramagnetic defects are produced, electron spin resonance can be a powerful technique. This is because in ESR technique, electrons are used as electric and magnetic microscopic probes. The defect concentration can be measured without difficulty, and the lowest detectable defect concentration is comparable with that of Levy's method. The integrated fast-neutron flux required is only 10^{14} to 10^{15} nV. At this low dose of irradiation, the simple model of independent (noninteracting) defects should be more reliable than at higher doses.

In a previous publication,³ we reported three kinds of paramagnetic centers in fast-neutron irradiated calcium tungstate. One of the centers, namely, the γ center, has been tentatively identified as due to paramagnetic tungsten associated with a nearest oxygen vacancy. In this paper, we will concentrate on this γ center alone. The arguments leading to this identification are presented. The number of defects is measured

* Supported in part by a grant from the National Aeronautics and Space Administration.

† Owens-Illinois Fellow.

¹ J. J. Antal, R. J. Weiss, and G. J. Dienes, *Phys. Rev.* **99**, 1081 (1955).

² P. W. Levy, *Phys. Rev.* **129**, 1076 (1963).

³ K. Chu and C. Kikuchi, *IEEE Trans. Nucl. Sci.* **NS-13**, 41 (1966).

and compared with the theoretical treatments due to Kinchin and Pease.

II. EXPERIMENTAL PROCEDURES

Samples and Orientations

Samples investigated were pure calcium-tungstate single crystals grown by the Czochralski method and obtained from the Harry Diamond Laboratories. Before irradiation, crystals showed a prominent spectrum of Mn^{2+} , although the concentration varied by as much as a factor of 10^2 , ranging from 10^{13} to 10^{16} spins per gram sample.

The crystals were oriented by x-ray diffraction and cemented to the end of quartz rods. The mounted crystals were then inserted into the microwave cavities at right angles to the static magnetic field. The quartz rod served as the axis for changing the crystal orientations.

ESR Measurements

ESR measurements were made by using an X-band (9.5-Gc/sec) spectrometer with 5-kc/sec modulation and a Ku-band (16.5-Gc/sec) spectrometer with 400-cps modulation. Ceramic cylindrical TE_{011} cavities with variable cross-coupling loops were used for both room-temperature and liquid-nitrogen-temperature measurements. A 12-in. Varian electromagnet with a 3.25-in. gap provided the magnetic field. The magnetic field was measured by using a Varian F-8 fluxmeter connected to a Berkeley 7800 transfer oscillator and a Berkeley 7370 universal EPUT.

Irradiations

The nuclear-reactor irradiations were made in the University of Michigan swimming-pool-type research reactor. Samples were placed in a small polyethylene bottle, using bismuth slugs as weights. In order to maximize the neutron flux, irradiations were carried out at a location close to the reactor core where the temperature was about 60°C . The fast- and thermal-neutron fluxes were 3×10^{12} n/cm^2 sec and 2.2×10^{13} n/cm^2 sec, respectively. Irradiation times from 20 min to 10 h were used. Longer irradiation times were not feasible, because of the excessive induced radioactivity of W^{185} and W^{187} . Most irradiations were done with the samples wrapped in cadmium cylinders of 30-mil thickness to minimize thermal-neutron-induced radioactivity. After irradiation, samples were removed from the reactor-core region to the side of the pool where the neutron flux was negligible. A waiting period from 3 to 15 days was necessary, depending on the irradiation time, before the samples could be taken out of the pool for measurement. X irradiations were made using a G.E. x-ray unit with a tungsten tube operating at 50-kV peak and 50 mA. The γ irradiations were made with a calibrated 10 000-Ci cobalt-60 source at the Phoenix Laboratory of the University of Michigan.

Uniaxial Stress

Uniaxial stress was applied to the sample up to 11 000 psi. The sample was placed on a cylinder of Teflon, which becomes quite hard at low temperature. A simple lever with a weight outside the Dewar supplied the force to the quartz rod, and on the other end of the quartz rod the oriented sample was cemented.

Concentration Measurement

For the determination of defect concentration, a sample was irradiated at a location where the neutron flux was measured for 1 h. The number of paramagnetic defects was determined by comparison with a standard copper-sulfate sample.

The difficulties encountered in measuring spin concentration, and the relative merits of several approaches to the problem, are discussed in Refs. 4–6. The method used here is similar to that of Singer and Kommandeur.⁴ Under proper conditions, the static spin susceptibility χ_0 is related to P , the power absorbed in an ESR experiment at magnetic field H , by the expression

$$\chi_0 = \frac{4\gamma}{\pi^2 \omega^2 H_1^2} \int_0^\infty P dH, \quad (1)$$

where ω is the angular frequency of the rf field, which has an amplitude H_1 inside the sample, and γ is the gyromagnetic ratio. It is related to the spectroscopic splitting factor g by $\gamma = g\beta/\hbar$.

This relationship holds if (a) the spin system is in thermal equilibrium with its surroundings, (b) the linewidth is small compared with the resonance field, (c) the modulation amplitude is small compared with the linewidth, and (d) the skin effect is absent.

The absence of saturation was verified by examining the signal height as a function of incident power. Examination of the linewidth of the γ centers showed that the second condition was met. The modulation amplitude was kept less than one-tenth of the linewidth (5 G). The symmetry of the signals showed the skin effect to be absent.

In practice, reference samples of known spin concentration were used, so that the spin susceptibilities and concentrations could be obtained for the expression

$$\frac{n}{n^*} = \frac{\chi}{\chi^*} = K \left(\frac{g}{g^*} \frac{S}{S^*} \frac{G}{G^*} \frac{H_m}{H_m^*} \right) \left(\frac{\Delta H}{\Delta H^*} \right)^2, \quad (2)$$

where n is the number of spins, g is the spectroscopic splitting factor, χ is the susceptibility, S is the signal height, G is the amplitude gain, H_m is the modulation

⁴ L. S. Singer and J. Kommandeur, J. Chem. Phys. **34**, 133 (1966).

⁵ R. H. Hoskins and R. C. Pastor, J. Appl. Phys. **31**, 1506 (1960).

⁶ R. T. Weidner and C. A. Whitmer, Phys. Rev. **91**, 1279 (1953).

amplitude, and ΔH is the linewidth. The asterisk values and unasterisk values pertain to the reference and the sample, respectively. K is a factor depending on the line shapes of the sample and the reference; $K=1$ if the line shapes are the same. If the reference is Lorentzian but the sample is Gaussian,⁵ then $K=0.29$. In order to determine K , a line-shape analysis was made for both the reference and the sample.

The method of line-shape analysis was similar to that used by Weidner and Whitmer⁶ for an absorption curve. If one measures the widths of an experimental derivative curve at various fractional heights and plots these widths against the width at the same fractional heights for some theoretical derivative curve, a straight-line result will indicate that the experimental and the theoretical curves have the same shape.

The reference sample used was $\text{CuSO}_4 \cdot 5\text{H}_2\text{O}$ in single-crystal form. Single crystals of convenient size (a few hundred micrograms) can be chosen directly from a reagent bottle of the chemical, weighed on an electrobalance, and then imbedded in paraffin. The standard sample was simply glued to the side of the CaWO_4 crystal during measurement. It has been reported that no change in the ESR properties was observed over a period of several years.⁷ The line shape of copper sulfate has been reported to be Lorentzian, and the shape of the γ center can be best fitted by 65% Gaussian and 35% Lorentzian. This gives $K=0.65+0.35 \times 0.29=0.75$.

III. RESULTS

Figure 1, shows a typical ESR spectrum at liquid-nitrogen temperature before and after reactor-neutron irradiation. The magnetic field is along the crystal c axis. The bottom trace is the spectrum before irradiation.

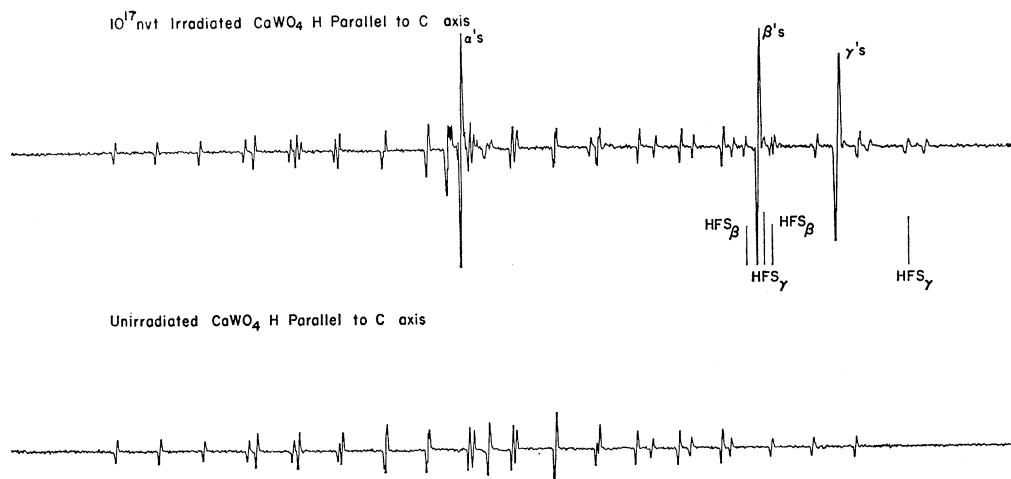


FIG. 1. CaWO_4 ESR spectrum before and after 10^{17} -nV neutron irradiation. $T=77^\circ\text{K}$. H parallel to the crystal c axis. Lines before irradiation are due to Mn^{++} impurity.

It is due to Mn^{2+} impurity, with concentration about 10^{16} spin/g. After irradiation, three groups of new lines are observed, denoted α , β , and γ . The α group is the only one which can be observed at room temperature. In general, it consists of four lines which merge into one along the c axis. The β group, in general, consists of two sets of three lines which merge into one set along the c axis. Each set consists of a central line flanked by two satellites with the intensity ratio 1:12:1; the weak lines are interpreted as the tungsten W^{183} hyperfine structure. The lines labeled HFS_β in Fig. 1 are these tungsten hyperfine lines. The separation along the c axis is 54 G. The γ group, in general, consists of four sets of three lines which merge into one set along the c axis. The three-line pattern is attributed to tungsten hyperfine structure. In Fig. 1, the hyperfine lines for the γ group are denoted by HFS_γ , with a separation of 280 G along the c axis. The principal values of the g tensors and the direction of the axes are shown in Table I and Fig. 2.

The arguments leading to the identification of the γ center as paramagnetic tungsten associated with an oxygen vacancy are as follows.

(1) Paramagnetic resonance signature: Each main line of the γ group is flanked by two satellites whose intensities are about $\frac{1}{12}$ that of the main line, the separation being 280 G along the c axis and 320 G along the $[110]$ direction. This relative intensity of 1:12:1 is expected for tungsten. The combined abundance of the even isotopes (W^{180} , W^{182} , W^{184} , W^{186}) is 85.6%. The odd isotope W^{183} , with $I=\frac{1}{2}$, has the abundance 14.4%, giving the expected relative intensities of 1:11.9:1.

(2) Angular dependence: Figure 3 shows the observed spectrum when the magnetic field is varied in the diagonal plane of the tungstate radical. The insert

⁷ L. S. Singer, J. Appl. Phys. 30, 1463 (1959).

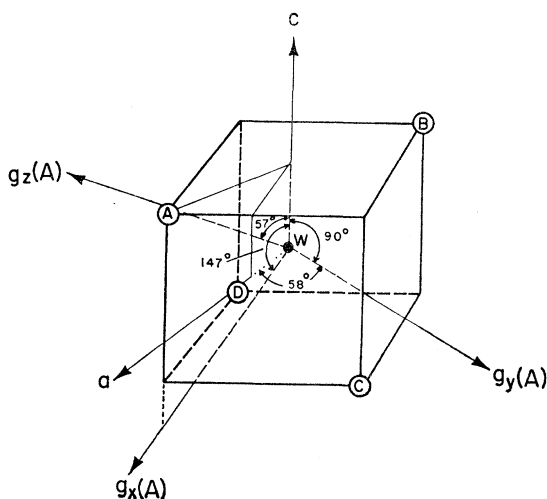
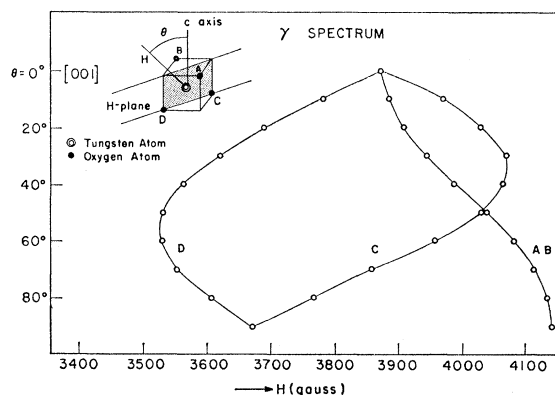
TABLE I. Principal values of the g tensors and the directions of the axes of the γ center.

	z	x	y
g	1.914	1.675	1.646
Δg	0.088	0.327	0.356
θ_A, θ_B	57°	147°	90°
φ_A	32°	32°	302°
φ_B	212°	212°	122°
θ_C, θ_D	123°	33°	90°
φ_C	302°	302°	32°
φ_D	122°	122°	212°

shows the central tungsten and four oxygens A , B , C , and D . If the magnetic field is in the diagonal (shaded) plane, the sites A and B become equivalent, so that a single ESR line is expected.

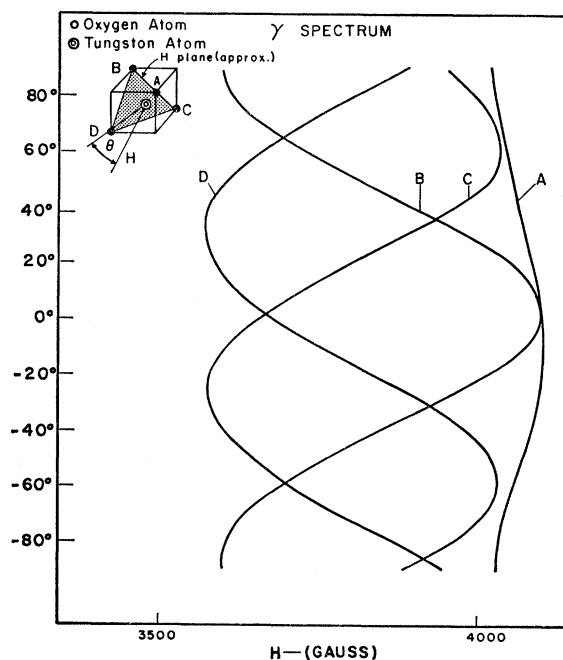
Similarly, Fig. 4 shows consistency between the expected and observed spectra when the magnetic field is varied in a plane normal to the W-O bond direction. Crystal data indicate that the polar angles for the direction of the A sites are $\theta=56^\circ 44'$ and $\varphi=31^\circ 54'$. The angles for the direction of one of the principal axes are $\theta=57^\circ$ and $\varphi=32^\circ$.

(3) Uniaxial stress: Experiment was carried out with a maximum stress at 11 000 psi along the $[110]$ direction of the crystal. In this case, two of the sites, namely, A and B , will make equal angles of 36° with the applied stress, but C and D will make equal angles of 79° with the applied stress. Thus it is expected that the effect of uniaxial stress is to change the intensities of A and B in one way and to change the intensities of C and D in another. Since the total number of defects is not changed by the stress, the change in intensity of A and B must be compensated by the change in intensity of C and D . This also has been confirmed experimentally.³

FIG. 2. Orientations of the principal axes of the γ -center g tensor.FIG. 3. Angular dependence of the γ lines. $T=77\text{K}$. H is varied in the shaded diagonal plane of the WO_4 bisphenoid.

(4) g Tensor: Table I gives the principal values of the g tensor. The largest g value, denoted by g_z , is (within experimental error) along the W-O bond direction. The second axis, labelled g_x , is in the same azimuthal plane, and the third axis, g_y , lies in the horizontal (ab) plane.

The small value of $\Delta g_z = -0.088$, compared with $\Delta g_x = -0.327$ and $\Delta g_y = -0.356$, is also consistent with the proposed defect model. In fact, for an equilateral arrangement of the three oxygens, Δg_z is expected to be zero, and $\Delta g_x \neq 0$, $\Delta g_y \neq 0$. In a field of C_{3v} symmetry, the $5d$ -orbital levels are expected to split into $A_1 + 2E$,

FIG. 4. Angular dependence of the γ lines. $T=77\text{K}$. H is varied in the shaded plane containing three oxygens of the WO_4 bisphenoid.

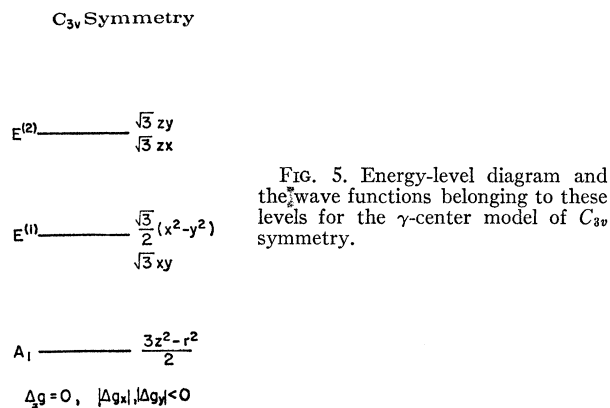


FIG. 5. Energy-level diagram and the wave functions belonging to these levels for the γ -center model of C_{3v} symmetry.

with the A_1 level lying lowest, as shown in Fig. 5. The A_1 level is nondegenerate, whereas the E is twofold degenerate. The wave functions belonging to these levels are as shown.

The experimental result that Δg_z is not exactly zero can be accounted for by noting that the three oxygens actually form an isosceles triangle, giving rise to a field of C_s symmetry. The levels contributing to Δg_z , Δg_x , and Δg_y are indicated in Fig. 6.

(5) Oxygen vacancy: The center giving the unique direction to the g tensor is an oxygen vacancy. The evidence for this is that the γ centers are produced by fast neutrons, but not by x rays, γ rays, and thermal neutrons. In addition, the centers anneal out completely if heated to 600°C for about 1 h.

The crystal structure of CaWO_4 is such that one oxygen is bonded to one tungsten only. Hence the number of γ centers is equivalent to the number of oxygen vacancies.

The γ centers are remarkably stable at room temperature, since no appreciable reduction in the ESR line intensity occurred over a four-week period. This is in contrast to the β centers, whose intensity is halved in the same period. The β centers, as indicated elsewhere,⁸ are attributed to paramagnetic tungsten associated with a calcium vacancy.

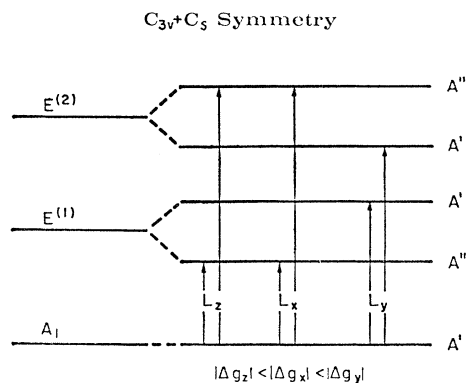


FIG. 6. Energy-level diagram and the allowed crystal-field transitions for the γ center of $C_{3v}+C_s$ symmetry.

Defect Concentration

The γ center is quite stable at room temperature, and no measurable annealing has been detected after heating up to 60°C for 1 h. In order to be able to compare the measured defect concentration with the theoretical work of Kinchin and Pease,⁸ the sample was irradiated for 1 h at a location where the neutron flux is known. The number of γ centers is obtained by comparison with a standard copper-sulfate sample.

The theoretical value for the number of atoms displaced may be calculated from the work of Kinchin and Pease.⁸ Their expression for the number of atoms displaced on the average for each neutron collision is

$$\bar{N}_v = (2 - L_c/E_{\max})L_c/4E_d. \quad (3)$$

Here E_d is the energy required for displacement of an

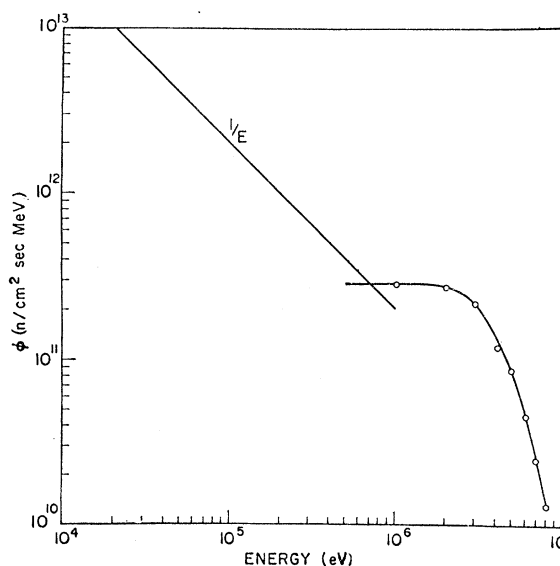


FIG. 7. Neutron-flux spectrum at the irradiation facility of the Ford Nuclear Reactor at the University of Michigan.

atom from its lattice site, taken here to be uniformly 25 eV; and E_{\max} is the maximum energy transferred to an atom by an impinging neutron, a quantity which depends upon the energy of the bombarding neutron and the masses of the neutron and the atom. L_c is the threshold energy for ionization and is given by⁹ $\frac{1}{2}(M/M_e)I$, where M is the mass of the moving atom, M_e is the mass of the electron, and I is the energy corresponding to the edge of the first main optical absorption band. For calcium tungstate, I is measured at 0.25μ . The number of fast-neutron collision per unit volume is given by

$$N_n = N\sigma_n\Phi,$$

where σ_n is the fast-neutron cross section per atom in

⁸ G. H. Kinchin and R. S. Pease, Rept. Progr. Phys. 18, 1 (1955).

⁹ F. Seitz, Discussions Faraday Soc. 5, 271 (1949).

the material, Φ is the neutron flux, and N is the number of atoms per unit volume.

The fast-neutron flux has been measured by Harris *et al.*,¹⁰ using a solid-state proton recoil telescope. The epithermal flux was measured by resonance-foil activation and absolute γ counting technique. The neutron-flux spectrum at the irradiation facility of the Ford Nuclear Reactor is shown in Fig. 7. Using these neutron-flux data and the neutron-cross-section data from Hughes and Schwartz,¹¹ viz., $\sigma(\text{O})=3$ b, $\sigma(\text{Ca})=3$ b, and $\sigma(\text{W})=10$ b, numerical integration of the Kinchin-Pease relation gives the calculated number of displacements. For a sample of 270 mg irradiated for 1 h, the calculated oxygen-vacancy concentration is 5.9×10^{16} displacements per gram. Using copper sulfate as standard and Eq. (2), the measured concentration is 5.0×10^{16} displacements per gram.

IV. DISCUSSION

The measurement of the so-called γ -center concentration provides one of the few opportunities for a

TABLE II. Principal axis directions and principal values of g tensors for the Zeldes-Livingston lines.

	Direction cosine			g
	a	b	c	
g_1	0.574(56°48')	-0.837(146°53')	0.008(89°31')	1.5716
g_2	0.832(32°39')	0.543(57°5')	-0.111(96°24')	1.6334
g_3	0.089(84°52')	0.068(86°4')	0.994(5°)	1.8482

comparison with radiation-damage theory. It is interesting to recall that in the literature,¹² except for a few cases, most of the experimentally measured defect concentrations are 5 to 10 times less than the theoretical values predicted by the simple radiation-damage theory.

Two additional tungsten centers have been reported in calcium tungstate, close to the centers reported here. Zeldes and Livingston¹³ reported a center produced by irradiating calcium tungstate at 77°K and indicated that it could be WO_4^{3-} near a lattice defect. The hyperfine interaction of their center varies from 35 to 65 G, and the principal axis directions and principal values of g tensors are shown in Table II.

¹⁰ L. Harris, Jr., G. Sherwood, and J. S. King, Nucl. Sci. Eng. **26**, 571 (1966).

¹¹ D. J. Hughes and R. B. Schwartz, Brookhaven National Laboratory Report No. BNL-325 (unpublished).

¹² G. Dienes and Vineyard, *Radiation Effects in Solids* (Interscience Publishers, Inc., New York, 1957).

¹³ H. Zeldes and R. Livingston, J. Chem. Phys. **34**, 247 (1961).

TABLE III. Fermi-contact-term effective field (H_c) for alkalis.

Atom	State	H_c (kG)
Li	$2s^2S$	122
Na	$3s^2S$	394
K	$4s^2S$	581
Rb	$5s^2S$	1229
Cs	$6s^2S$	1513

Azarbayejani¹⁴ reported a center in vacuum-reduced $\text{CaWO}_4:\text{Y}$. The parameters for $\mathbf{H} \perp c$ are $g_1=1.587$, $g_2=1.600$, $A_1=53.3$ G, $A_2=66.3$ G, and for $\mathbf{H} \parallel c$ the values are $g=1.850$, $A=19.5$ G. These results strongly suggest that the centers reported by the two groups of investigators (Zeldes and Livingston, and Azarbayejani) are undisturbed WO_4^{3-} associated with a lattice defect.

In the case of the β center, we have $g_1=1.791$, $g_2=1.724$, $A_1=54$ G, $A_2=120$ G when $\mathbf{H} \perp c$; and $g=1.801$, $A=51$ G when $\mathbf{H} \parallel c$. The identification of β centers as undisturbed WO_4^{3-} with a nearest-calcium displacement is apparently consistent with the two reported tungsten centers by Zeldes and Azarbayejani. The γ center, on the other hand, is evidently of a different nature. The g and A tensors are very different from the three kinds of centers just mentioned. This is because the γ center consists of a WO_4^{3-} with one of the four oxygens displaced.

The large hyperfine interaction of the γ center seems unusual, considering the small nuclear magnetic moment of W^{183} ($\mu=0.155\mu_N$). Yafaev and Garifyanov¹⁵ reported an A value of 240 G in glass. For the γ center, the A value varies from 280 to 320 G. These values are not inconsistent with the assumption that there is a considerable admixture of the $6S$ state for which the Fermi-contact effective field is very large, as shown in Table III.¹⁶

ACKNOWLEDGMENTS

We wish to thank David Mason and Clyde Morrison for many helpful discussions. In addition, one of us (K.C.C.) gratefully acknowledges support by a grant from the Owens-Illinois Glass Company of Toledo, Ohio.

¹⁴ G. H. Azarbayejani, Bull. Am. Phys. Soc. **10**, 1131 (1965).

¹⁵ N. R. Yafaev and N. S. Garifyanov, Fiz. Tverd. Tela [English transl.: Soviet Phys.—Solid State **6**, 269 (1963)].

¹⁶ N. Ramsey, *Nuclear Moments* (John Wiley & Sons, Inc., New York, 1953).